Time-dependent close-coupling calculations of correlated photoionization processes in helium

M. S. Pindzola and F. Robicheaux
Department of Physics, Auburn University, Auburn, Alabama 36849
(Received 29 July 1997)

Various correlated photoionization processes in helium are calculated by direct solution of the time-dependent Schrödinger equation. An inhomogeneous set of time-dependent close-coupled partial differential equations are partitioned on a numerical lattice for easy implementation on massively parallel computers. Projection of the time evolved wave function onto lattice eigenstates for He^+ yields cross sections for photoionization with excitation and double photoionization. The computational results are compared with recent experimental measurements. [S1050-2947(98)07701-4]

PACS number(s): 32.80.Fb

I. INTRODUCTION

An accurate description of the correlation between two electrons moving in the long-range Coulomb field of a third body, as found in the double photoionization of helium, remains a challenging theoretical problem. However, the difficulties are somewhat mitigated if examined in the time domain. As pointed out by Bottcher [1], the time evolution of a wave function localized in space, as found in the ground state of helium, obviates the need for answers to questions about the asymptotic form of the wave function in coordinate space or its singularities in momentum space. In this paper a time-dependent close-coupling method [2,3] developed to study the electron-impact ionization of atomic ions [4] has been extended to include radiative dipole coupling. This larger set of coupled partial differential equations may then be time propagated on a lattice to yield accurate cross sections for a variety of correlated photoionization processes in two-electron atomic systems.

We begin with test calculations for the photoionization of ground-state helium above the complete fragmentation threshold. Recent synchrotron light experiments have narrowed the measurement uncertainties both for photoionization with excitation [5] and double photoionization [6–8] of ground-state helium so as to provide benchmarks for the development of new theoretical methods. Additional comparisons may be made with the vast number of time-independent computational theories developed to understand correlated processes in the photoionization of helium. The most popular methods for photoionization with excitation are based on many-body perturbation theory [9,10] and standard R-matrix theory [11,12]. Recent calculations for double photoionization, which involve the full three-body Coulomb breakup, have been based on many-body perturbation theory [13–16], initial-state dipole response functions [17–19], asymptotically correlated final states [20–24], hyperspherical [25] and convergent [26] close-coupling theory, and eigenchannel [27,28] and Laguerre pseudostate [29] R-matrix theory. In the following paragraphs we first develop the time-dependent close-coupling method as applied to the photoionization of two-electron atoms in Sec. II, compare our test results for ground-state helium with experiment in Sec. III, and then give a brief summary in Sec. IV.

II. THEORY

The time-dependent wave function for any two-electron atomic system may be divided into two parts:

$$\Psi(\vec{r}_1,\vec{r}_2,t)=\phi_0(\vec{r}_1,\vec{r}_2)e^{-iE_0t}+\psi(\vec{r}_1,\vec{r}_2,t), \tag{1}$$

where ϕ_0 is the exact eigenfunction and E_0 is the exact eigenenergy of the time-independent atomic Hamiltonian. Substitution into the time-dependent Schrödinger equation yields (in atomic units)

$$i\frac{\partial\psi(\vec{r}_1,\vec{r}_2,t)}{\partial t}=(H_{\rm atom}+H_{\rm rad})\psi(\vec{r}_1,\vec{r}_2,t)+H_{\rm rad}\phi_0(\vec{r}_1,\vec{r}_2)e^{-iE_0t}, \tag{2}$$

where $H_{\rm rad}$ is the Hamiltonian for interaction with a time-dependent radiation field. In the weak-field perturbative limit, one may solve the somewhat simpler time-dependent equation given by

$$i\frac{\partial\psi(\vec{r}_1,\vec{r}_2,t)}{\partial t}=H_{\rm atom}\psi(\vec{r}_1,\vec{r}_2,t)+H_{\rm rad}\phi_0(\vec{r}_1,\vec{r}_2)e^{-iE_0t}. \tag{3}$$

The second term on the right-hand side acts as a source for the time evolution of $\psi(\vec{r}_1,\vec{r}_2,t)$ from zero at time $t=0$ to some final value at time $t=T$. This inhomogeneous time-dependent equation is the photoabsorption analog of the time-dependent Green's function method [30] introduced for electron-impact ionization of atoms. The equation is also similar in spirit to the time-independent dipole response function method [17–19] in that only outgoing waves are generated. As shown below in some detail, cross sections for a variety of photoionization processes may be easily extracted from the final wave function $\psi(\vec{r}_1,\vec{r}_2,T)$.

Utilizing a standard procedure found in time-independent scattering theory [31–33], the time-dependent wave function for a given LS symmetry is expanded in coupled spherical harmonics:

$$\psi(\vec{r}_1,\vec{r}_2,t)=\sum_{L,S}\sum_{l_1,l_2}\frac{P^{LS}_{l_1l_2}(r_1,r_2,t)}{r_1r_2}Y^L_{l_1l_2}(\hat{r}_1,\hat{r}_2), \tag{4}$$

where l_1 and l_2 are the angular momenta of the two electrons, and L and S are the total orbital and spin angular momenta of the atomic system. Upon substitution into Eq. (3), the time-dependent close-coupled radial partial differential equations are given by

$$i\frac{\partial P^{LS}_{\ell_1\ell_2}(r_1,r_2,t)}{\partial t}=T_{\ell_1\ell_2}(r_1,r_2)P^{LS}_{\ell_1\ell_2}(r_1,r_2,t)+\sum_{\ell_1',\ell_2'}V^{L}_{\ell_1\ell_2,\ell_1'\ell_2'}(r_1,r_2)P^{LS}_{\ell_1'\ell_2'}(r_1,r_2,t)$$
$$+\sum_{\ell_1'',\ell_2''}W^{LL_0}_{\ell_1\ell_2,\ell_1''\ell_2''}(r_1,r_2,t)P^{L_0S}_{\ell_1''\ell_2''}(r_1,r_2)e^{-iE_0t}, \tag{5}$$

where

$$T_{\ell_1\ell_2}(r_1,r_2)=-\frac{1}{2}\frac{\partial^2}{\partial r_1^2}-\frac{1}{2}\frac{\partial^2}{\partial r_2^2}+\frac{\ell_1(\ell_1+1)}{2r_1^2}+\frac{\ell_2(\ell_2+1)}{2r_2^2}-\frac{Z}{r_1}-\frac{Z}{r_2}, \tag{6}$$

$P^{L_0S}_{\ell_1,\ell_2}(r_1,r_2)$ are the radial wave functions for the initial wave function ϕ_0, and Z is the atomic number. The Coulomb interaction operator is given by [34]

$$V^{L}_{\ell_1\ell_2,\ell_1'\ell_2'}(r_1,r_2)=(-1)^{L+\ell_2+\ell_2'}\sqrt{(2\ell_1+1)(2\ell_1'+1)(2\ell_2+1)(2\ell_2'+1)}$$
$$\times\sum_{\lambda}\frac{r_<^{\lambda}}{r_>^{\lambda+1}}\begin{pmatrix}\ell_1 & \lambda & \ell_1'\\ 0 & 0 & 0\end{pmatrix}\begin{pmatrix}\ell_2 & \lambda & \ell_2'\\ 0 & 0 & 0\end{pmatrix}\begin{Bmatrix}L & \ell_2' & \ell_1'\\ \lambda & \ell_1 & \ell_2\end{Bmatrix}, \tag{7}$$

where $r_<=\min(r_1,r_2)$ and $r_>=\max(r_1,r_2)$. The selection rules of the $3j$ and $6j$ symbols limit the multipole expansion to a small number of terms. The radiation field operator is given by [34]

$$W^{LL'}_{\ell_1\ell_2,\ell_1',\ell_2'}(r_1,r_2,t)=\delta_{\ell_2,\ell_2'}(-1)^{\ell_2}\sqrt{(2\ell_1+1)(2\ell_1'+1)(2L+1)(2L'+1)}$$
$$\times g(r_1)F(t)\begin{pmatrix}\ell_1 & 1 & \ell_1'\\ 0 & 0 & 0\end{pmatrix}\begin{pmatrix}L & 1 & L'\\ 0 & 0 & 0\end{pmatrix}\begin{Bmatrix}\ell_1 & \ell_2 & L\\ L' & 1 & \ell_1'\end{Bmatrix}$$
$$+\delta_{\ell_1,\ell_1'}(-1)^{\ell_1}\sqrt{(2\ell_2+1)(2\ell_2'+1)(2L+1)(2L'+1)}$$
$$\times g(r_2)F(t)\begin{pmatrix}\ell_2 & 1 & \ell_2'\\ 0 & 0 & 0\end{pmatrix}\begin{pmatrix}L & 1 & L'\\ 0 & 0 & 0\end{pmatrix}\begin{Bmatrix}\ell_2 & \ell_1 & L\\ L' & 1 & \ell_2'\end{Bmatrix}. \tag{8}$$

The time dependence of the linearly polarized electric field is given by

$$F(t)=f(t)\cos(\omega t), \tag{9}$$

where the ramp function $f(t)=t/T$ for $t<T/4$, $f(t)=1$ for $t>T/4$. In the length gauge

$$g(r)=r, \tag{10}$$

while in the velocity gauge

$$g(r)=\frac{i}{\omega}\left(\frac{\partial}{\partial r}+\frac{\ell'(\ell'+1)-\ell(\ell+1)}{2r}\right), \tag{11}$$

where ω is the frequency of the radiation field. We note that coupled spherical harmonic expansions may also be substituted into Eq. (2), yielding a set of time-dependent close-coupled radial partial differential equations similar to those used by Parker *et al.* [35] to study intense-field multiphoton ionization of two-electron atoms.

We solve the time-dependent close-coupled equations using lattice techniques to obtain a discrete representation of the radial wave functions and all operators on a two-dimensional grid. For easy implementation on massively parallel computers, low-order finite difference methods are employed with uniform mesh spacing. For example, the kinetic energy has a lattice representation in terms of a tridiagonal matrix, while the Coulomb interaction operator becomes a diagonal matrix. We divide the radial wave functions as follows:

$$P^{LS}_{\ell_1\ell_2}(r_1,r_2,t)\neq 0 \quad \text{for } 0<r_1<R, \quad \frac{(j-1)R}{N}<r_2<\frac{jR}{N} \tag{12}$$

with each strip $j=1,2,...,N$ on a separate processor. To evaluate first and second derivatives, one only needs to pass $P^{LS}_{\ell_1,\ell_2}(r_1,r_2=(j-1)R/N,t)$ to processor $(j-1)$ for $j=2,3,\ldots,N$ and $P^{LS}_{\ell_1,\ell_2}(r_1,r_2=jR/N,t)$ to processor $(j+1)$ for $j=1,2,\ldots,(N-1)$.

The eigenfunctions ϕ_n and eigenenergies E_n for the ground and low-lying excited states of any two-electron atomic system may be found by relaxation of the Schrödinger equation in imaginary time $(\tau=it)$ [36]:

$$-\frac{\partial\phi_n(\vec{r}_1,\vec{r}_2,\tau)}{\partial\tau}=H_{\text{atom}}\phi_n(\vec{r}_1,\vec{r}_2,\tau). \tag{13}$$

For a given LS symmetry, $\phi_n(\vec{r}_1,\vec{r}_2,\tau)$ may be expanded in coupled spherical harmonics resulting in a coupled set of radial partial differential equations. An explicit exponential time propagator is used to ''relax'' an initial guess to the lowest eigenenergy for that symmetry. A spectrum of excited states may then be built up with successive relaxations with projection.

The eigenfunctions χ_n and eigenenergies ϵ_n for the ground and all bound and continuum excited states of any one-electron atomic system may be found by direct diagonalization of the time-independent Schrödinger equation:

$$h_{\text{atom}}\chi_n(\vec{r})=\epsilon_n\chi_n(\vec{r}). \tag{14}$$

For a given orbital angular momentum, $\chi_n(\vec{r})$ may be written as a product of a radial function and a spherical harmonic resulting in an uncoupled set of ordinary differential equations. Each radial equation is diagonalized on a one-dimensional grid; the same uniform mesh as used for the two-electron atomic system. The number of eigenfunctions and eigenenergies for each angular momentum equals the total number of lattice points.

After calculation of the two-electron eigenfunction for the initial atom ϕ_0 and the one-electron eigenfunctions for the final ion, χ_n, the time-dependent close-coupled equations found in Eq. (5) are propagated in real time for the appropriate LS symmetry and the initial condition: $P^{LS}_{\ell_1,\ell_2}(r_1,r_2,t=0)=0$. An explicit ''staggered leapfrog'' approximation [37] is used for time propagation. The method is ideal for massively parallel computers since it involves only simple matrix-vector multiplications at each time step. The norm of the wave function continues to grow in a strict linear manner if we adjust the time step to be less than one divided by the eigenvalue with largest absolute value of the discrete Hamiltonian operator.

To extract cross sections from the time evolved radial wave functions, we use standard projection techniques [38,39]. The probability of ionization with excitation to a bound state $n\ell m$ is given by

$$\begin{aligned}\wp^{LS}_{n\ell m}=&\int d\vec{r}_1\left|\langle\psi^{LS}(\vec{r}_1,\vec{r}_2,T)|\chi_{n\ell m}(\vec{r}_2)\rangle\right|^2\\&-\sum_{n'\ell'm'}\left|\langle\psi^{LS}(\vec{r}_1,\vec{r}_2,T)|\chi_{n'\ell'm'}(\vec{r}_1)\chi_{n\ell m}(\vec{r}_2)\rangle\right|^2\\&+\int d\vec{r}_2\left|\langle\psi^{LS}(\vec{r}_1,\vec{r}_2,T)|\chi_{n\ell m}(\vec{r}_1)\rangle\right|^2\\&-\sum_{n'\ell'm'}\left|\langle\psi^{LS}(\vec{r}_1,\vec{r}_2,T)|\chi_{n\ell m}(\vec{r}_1)\chi_{n'\ell'm'}(\vec{r}_2)\rangle\right|^2.\end{aligned} \tag{15}$$

The cross section for photoionization with excitation to a bound state $n\ell m$ is given by

$$\sigma^{LS}_{n\ell m}=\frac{\omega}{I}\frac{\partial\wp^{LS}_{n\ell m}}{\partial t}, \tag{16}$$

where I is the intensity of the radiation field. The probability for double ionization is given by

$$\begin{aligned}\wp^{LS}_{\text{dion}}=&\langle\psi^{LS}(\vec{r}_1,\vec{r}_2,T)|\psi^{LS}(\vec{r}_1,\vec{r}_2,T)\rangle-\sum_{n\ell m}\wp^{LS}_{n\ell m}\\&-\sum_{n\ell m}\sum_{n'\ell'm'}\left|\langle\psi^{LS}(\vec{r}_1,\vec{r}_2,T)|\chi_{n'\ell'm'}(\vec{r}_1)\chi_{n\ell m}(\vec{r}_2)\rangle\right|^2,\end{aligned} \tag{17}$$

while the cross section for double photoionization is given by

$$\sigma^{LS}_{\text{dion}}=\frac{\omega}{I}\frac{\partial\wp^{LS}_{\text{dion}}}{\partial t}. \tag{18}$$

We note that Eqs. (16) and (18) relate the cross section to a rate divided by the photon flux.

III. RESULTS

The time-dependent close-coupled (TDCC) equations are solved for the photoionization of helium in its ground state for photon energies ranging from 90 to 200 eV, well above the complete fragmentation threshold. We employ two lattices: one with 200×200 points and one with 400×400 points. Each radial direction from 0 to 40 is spanned

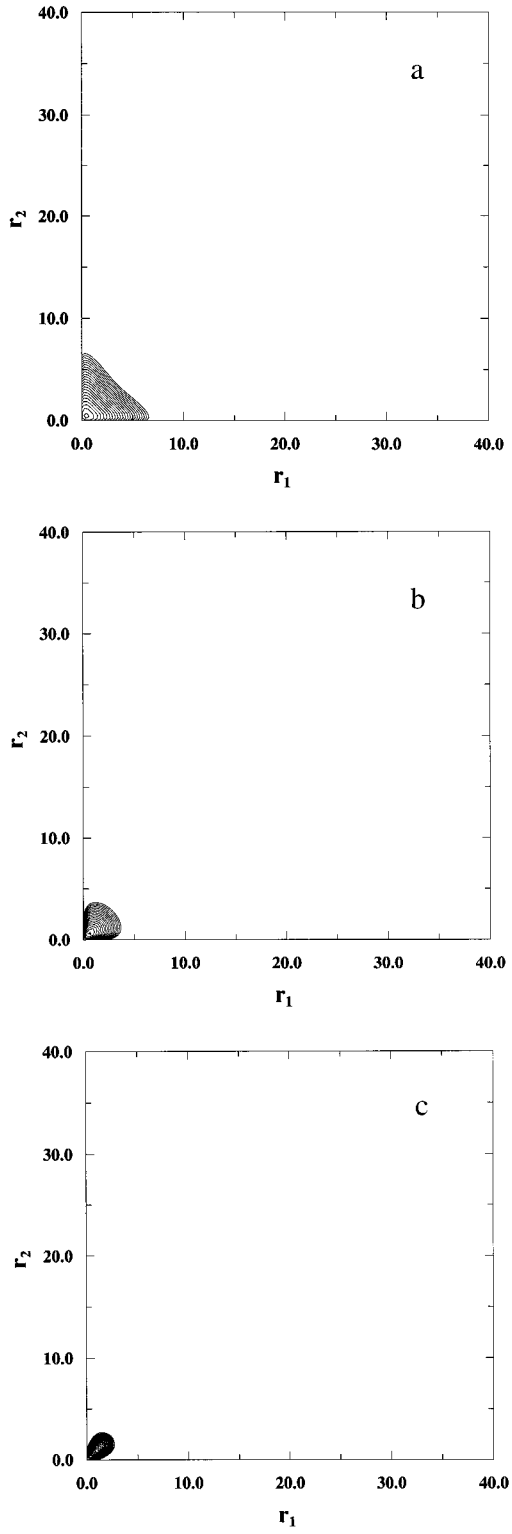

FIG. 1. Probability densities for the three channel ground state of helium, (a) ss channel, (b) pp channel, and (c) dd channel.

by a uniform mesh; on the first lattice the mesh spacing is $\Delta r = 0.2$, while on the second lattice $\Delta r = 0.1$.

Three coupled channels ($\ell_1\ell_2 = ss, pp, dd$) are sufficient to obtain a fully correlated ^1S ground state of helium on either lattice. After expanding Eq. (13) in coupled spherical harmonics, the Schrödinger equation in imaginary time has the form

TABLE I. Bound-state lattice eigenenergies for He^+.

nl	Energy (eV) 200 points	Energy (eV) 400 points
$1s$	−52.405	−53.890
$2s$	−13.472	−13.572
$2p$	−13.652	−13.617
$3s$	−6.020	−6.040
$3p$	−6.068	−6.052
$3d$	−6.049	−6.048
$4s$	−3.393	−3.399
$4p$	−3.412	−3.404
$4d$	−3.403	−3.402
$4f$	−3.402	−3.402
$5s$	−2.173	−2.176
$5p$	−2.183	−2.178
$5d$	−2.178	−2.177
$5f$	−2.177	−2.177
$6s$	−1.464	−1.464
$6p$	−1.477	−1.472
$6d$	−1.483	−1.481
$6f$	−1.494	−1.493
$7s$	−0.753	−0.749
$7p$	−0.789	−0.779
$7d$	−0.833	−0.827
$7f$	−0.897	−0.893

$$-\frac{\partial P^{00}_{\ell_1\ell_2}(r_1,r_2,\tau)}{\partial\tau} = T_{\ell_1\ell_2}(r_1,r_2)P^{00}_{\ell_1\ell_2}(r_1,r_2,\tau) + \sum_{\ell_1',\ell_2'} V^0_{\ell_1\ell_2,\ell_1'\ell_2'}(r_1,r_2)P^{00}_{\ell_1'\ell_2'}(r_1,r_2,\tau). \tag{19}$$

Relaxation of a trial function on the 200×200 lattice yields a ground-state wave function with probability density as shown in Fig. 1 and with an energy of -2.785 a.u. A 400×400 lattice calculation yields a similar density plot and an energy of -2.871 a.u. Further improvements in the absolute value of the total energy of ground-state helium (chemical accuracy is -2.904 a.u.) could be achieved by smaller mesh spacing and the use of higher-order differencing operators [40]. However, as will be shown below, it appears that the initial-state correlation retained in these ground-state lattice wave functions is sufficient for our purposes.

The lattice wave functions for He^+ are obtained by direct diagonalization of the radial Schrödinger equation associated with Eq. (14). The bound-state energies for a 200-point and a 400-point radial mesh are given in Table I. The box radius of 40 only supports spectroscopic states for $n\leqslant5$. The bound states for $n>5$ contain some continuum character, whereas the low-energy continuum box states contain some bound character. We note that the total cross-section expressions found in Eqs. (15)–(18) require only bound-state projections.

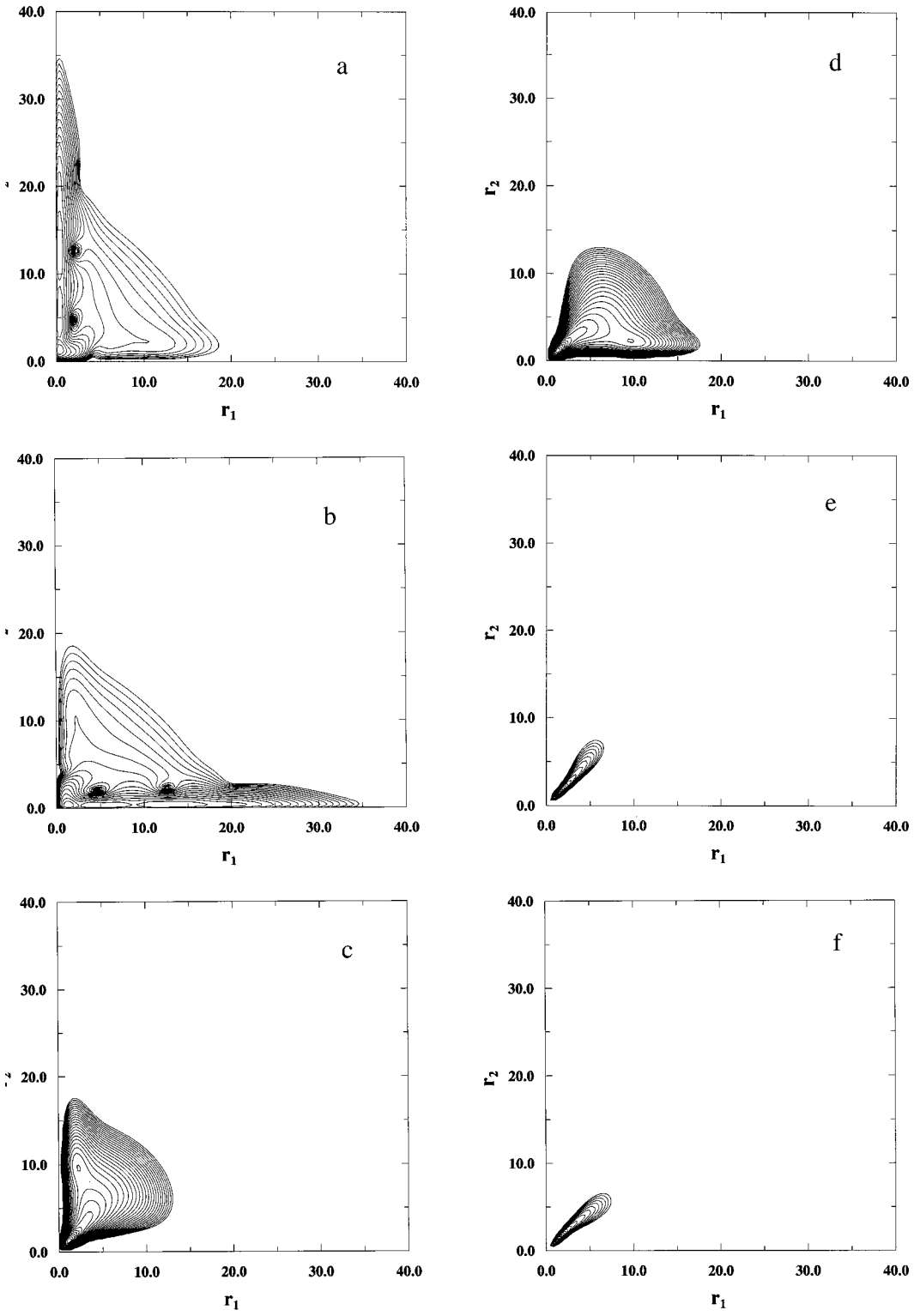

FIG. 2. Probability densities for the six-channel photoionization of helium at $t=\frac{1}{2}T$, (a) sp channel, (b) ps channel, (c) pd channel, (d) dp channel, (e) df channel, and (f) fd channel.

We retain six coupled channels ($\ell_1\ell_2 = sp,ps,pd,dp,df,fd$) in solving Eq. (5) for the photoionization of ground-state helium. For the 200×200 lattice the time step is $\Delta t=0.005$, while for the 400×400 lattice the time step is $\Delta t=0.001$. The total propagation time is $T=\frac{3}{2}R/\sqrt{2(\omega-\Delta)}$, where Δ is the single photoionization threshold. This guarantees that the first photoelectron that is ionized does not have time to reflect from the box boundary R and return far enough to disturb the second electron. For a photon energy $\omega=85$ eV on the 200×200 lattice, the probability density is shown in Fig. 2 for the six-channel wave function at time $t=\frac{1}{2}T$. The sp and ps channels are strongly dominated by single photoionization, whose density flow is nearing the boundary. Besides monitoring the probability

TABLE II. Ratio of photoionization with $n=2$ excitation to single photoionization for helium.

ω (eV)	TDCC $\Delta r=0.2$	TDCC $\Delta r=0.1$	Experiment [5] (error)
89.5	8.17%	7.60%	8.17% (0.04)
100.0	7.78%	7.23%	7.63% (0.04)
120.0	7.32%	6.78%	6.96% (0.05)
160.0	6.84%	6.27%	6.39% (0.10)
197.7	6.67%	5.96%	5.91% (0.06)

TABLE III. Ratio of photoionization with $n=3$ excitation to single photoionization for helium.

ω (eV)	TDCC $\Delta r=0.2$	TDCC $\Delta r=0.1$	Experiment [5] (error)
89.5	1.56%	1.46%	1.51% (0.03)
100.0	1.41%	1.33%	1.38% (0.03)
120.0	1.24%	1.16%	1.16% (0.03)
160.0	1.06%	0.98%	0.96% (0.04)
197.7	0.98%	0.88%	0.85% (0.04)

TABLE IV. Ratio of double photoionization to single photoionization for helium.

ω (eV)	TDCC $\Delta r=0.2$	TDCC $\Delta r=0.1$	Experiment [6] (error)	Experiment [7] (error)
90.0	2.12%	1.69%	2.45% (0.04)	1.66% (0.02)
120.0	3.94%	3.59%	3.66% (0.13)	3.26% (0.03)
140.0	4.31%	4.00%	3.91% (0.05)	3.70% (0.03)
160.0	4.52%	4.17%	4.14% (0.06)	3.89% (0.03)
190.0	4.50%	4.23%	4.20% (0.05)	3.97% (0.04)

TABLE V. Ratio of double photoionization to single photoionization for helium.

ω (eV)	TDCC $\Delta r=0.2$	TDCC $\Delta r=0.1$	Experiment [8] (error)
90.0	2.12%	1.69%	1.40% (0.05)
100.0	3.04%	2.65%	2.28% (0.05)
130.0	4.16%	3.84%	3.23% (0.07)
175.0	4.51%	4.22%	3.70% (0.07)
200.0	4.61%	4.22%	3.60% (0.08)

density, we also calculate the probabilities $\wp^{10}_{n\not=m}$ and $\wp^{10}_{\rm dion}$ at intermediate times. After an initial turn on from zero, all the probabilities become a linear function of time for $t>\frac{1}{2}T$. The slopes are extracted and the cross sections are computed from Eqs. (16) and (18).

Cross-section ratios for photoionization with excitation of helium are compared with a recent experiment by Wehlitz *et al.* [5] in Tables II and III. The ratios are found from summing over the degenerate levels for each n and then are expressed as a percentage of the single photoionization cross section at that photon energy. Although the 400×400 lattice calculations are slightly under experiment at low energies, the agreement by 200 eV is quite good. The many-body perturbation theory results of Chang [9] cross our 400×400 lattice calculations around 120 eV, being slightly higher at low energies and slightly lower at high energies.

Cross-section ratios for double photoionization of helium are compared with the recent experiments of Levin, Armen, and Sellin [6,7] and Dorner *et al.* [8] in Tables IV and V. Although the 400×400 lattice calculations agree quite well with the experiments of Levin, Armen, and Sellin [6], they are about 15% higher than the experiments of Dorner *et al.* [8] and the more recent experiments reported by Levin [7]. All the time-independent close-coupling calculations [25–28] lie between the Levin, Armen, and Sellin [6] and Dorner *et al.* [8] experimental measurements.

All the time-dependent close-coupling results presented in Tables II–V were calculated in the length gauge of Eq. (10). Spot calculations at 89.5 and 200 eV in the velocity gauge of Eq. (11) on both lattices produced cross-section ratios in excellent agreement with the length gauge results. It appears that the lattice calculations are almost gauge invariant.

IV. SUMMARY

Overall the time-dependent close-coupling calculations for the photoionization of helium agree well with the recent synchrotron light experiments. Improvements in the accuracy of these test calculations can be made by a combination of smaller lattice spacing, higher-order differencing, and larger boundary radius. Convergence studies are now possible on the most powerful massively parallel computers (like the Cray T3E). In the future we plan to apply the time-dependent lattice method to study photoionization of excited-state He, as well as ground-state H^- and Li^+. Inclusion of the radiation Hamiltonian in the time evolved wave function, along with the incorporation of fast electron absorbing boundary conditions, may also allow a detailed study of correlated multiphoton absorption processes in atoms.

ACKNOWLEDGMENTS

In this work, M.S.P. was supported in part by NSF Grant No. NSF-PHY-9122199 and F.R. was supported in part by NSF Young Investigator Grant No. NSF-PHY-9457903, both with Auburn University. We would like to thank both J. C. Levin and R. Dorner for providing us with their experimental measurements for helium in numerical form. Most of the computational work was carried out at the National Energy Research Supercomputer Center in Berkeley, California and the Center for Computational Sciences in Oak Ridge, Tennessee.

[1] C. Bottcher, Adv. At. Mol. Phys. **20**, 241 (1985).
[2] M. S. Pindzola and D. R. Schultz, Phys. Rev. A **53**, 1525 (1996).
[3] M. S. Pindzola and F. Robicheaux, Phys. Rev. A **54**, 2142 (1996).
[4] M. S. Pindzola, F. Robicheaux, N. R. Badnell, and T. W. Gorczyca, Phys. Rev. A **56**, 1994 (1997).
[5] R. Wehlitz, I. A. Sellin, O. Hemmers, S. B. Whitfield, P. Glans, H. Wang, D. W. Lindle, B. Langer, N. Berrah, J. Viefhaus, and U. Becker, J. Phys. B **30**, L51 (1997).
[6] J. C. Levin, G. B. Armen, and I. A. Sellin, Phys. Rev. Lett. **76**, 1220 (1996).
[7] J. C. Levin (private communication).
[8] R. Dorner, T. Vogt, V. Mergel, H. Khemliche, S. Kravis, C. L. Cocke, J. Ullrich, M. Unverzagt, L. Spielberger, M. Damrau, O. Jagutzki, I. Ali, B. Weaver, K. Ullmann, C. C. Hsu, M. Jung, E. P. Kanter, B. Sonntag, M. H. Prior, E. Rotenberg, J. Denlinger, T. Warwick, S. T. Manson, and H. Schmidt-Bocking, Phys. Rev. Lett. **76**, 2654 (1996).
[9] T. N. Chang, J. Phys. B **13**, L551 (1980).
[10] S. Salomonson, S. L. Carter, and H. P. Kelly, Phys. Rev. A **39**, 5111 (1989).
[11] V. L. Jacobs and P. G. Burke, J. Phys. B **5**, L67 (1972).
[12] K. A. Berrington, P. G. Burke, W. C. Fon, and K. T. Taylor, J. Phys. B **15**, L603 (1982).
[13] S. L. Carter and H. P. Kelly, Phys. Rev. A **24**, 170 (1981).
[14] K. Hino, T. Ishihara, F. Shimizu, N. Toshima, and J. H. McGuire, Phys. Rev. A **48**, 1271 (1993).
[15] K. Hino, P. M. Bergstrom, and J. H. Macek, Phys. Rev. Lett. **72**, 1620 (1994).
[16] C. Pan and H. P. Kelly, J. Phys. B **28**, 5001 (1995).
[17] D. Proulx and R. Shakeshaft, Phys. Rev. A **48**, R875 (1993).
[18] M. Pont and R. Shakeshaft, J. Phys. B **28**, L571 (1995).
[19] R. C. Forrey, Z. C. Yan, H. R. Sadeghpour, and A. Dalgarno, Phys. Rev. Lett. **78**, 3662 (1997).
[20] F. Maulbetsch and J. S. Briggs, Phys. Rev. Lett. **68**, 2004 (1992).
[21] Z. Teng and R. Shakeshaft, Phys. Rev. A **47**, R3487 (1993).
[22] L. R. Andersson and J. Burgdorfer, Phys. Rev. Lett. **71**, 50 (1993).
[23] K. Hino, Phys. Rev. A **47**, 4845 (1993).
[24] M. A. Kornberg and J. E. Miraglia, Phys. Rev. A **48**, 3714 (1993).
[25] J. Z. Tang and I. Shimamura, Phys. Rev. A **52**, R3413 (1995).
[26] A. S. Kheifets and I. Bray, Phys. Rev. A **54**, R995 (1996).
[27] K. W. Meyer and C. H. Greene, Phys. Rev. A **50**, R3573 (1994).
[28] K. W. Meyer, C. H. Greene, and B. D. Esry, Phys. Rev. Lett. **78**, 4902 (1997).
[29] T. W. Gorczyca and N. R. Badnell, J. Phys. B **30**, 3897 (1997).
[30] F. Robicheaux, M. S. Pindzola, and D. R. Plante, Phys. Rev. A **55**, 3573 (1997).
[31] A. Temkin, Phys. Rev. **126**, 130 (1962).
[32] J. Shertzer and J. Botero, Phys. Rev. A **49**, 3673 (1994).
[33] Y. D. Wang and J. Callaway, Phys. Rev. A **50**, 2327 (1994).
[34] R. D. Cowan, *The Theory of Atomic Structure and Spectra* (University of California Press, Berkeley, 1981), Chap. 11.
[35] J. Parker, K. T. Taylor, C. W. Clark, and S. Blodgett-Ford, J. Phys. B **29**, L33 (1996).
[36] S. E. Koonin, *Computational Physics* (Benjamin-Cummings, New York, 1986), Chap. 7.
[37] W. H. Press, S. A. Teukolsky, W. T. Vetterling, and B. P. Flannery, *Numerical Recipes* (Cambridge University Press, Cambridge, England, 1992), p. 833.
[38] R. Grobe and J. H. Eberly, Phys. Rev. A **47**, R1605 (1993).
[39] W. Ihra, M. Draeger, G. Handke, and H. Friedrich, Phys. Rev. A **52**, 3752 (1995).
[40] C. Bottcher, D. R. Schultz, and D. H. Madison, Phys. Rev. A **49**, 1714 (1994).